Available online at www.sciencedirect.com
ScienceDirect
International Journal of Non-Linear Mechanics 42 (2007) 1186–1193
INTERNATIONAL JOURNAL OF NON-LINEAR MECHANICS
www.elsevier.com/locate/nlm

Low-frequency band gaps in chains with attached non-linear oscillators

B.S. Lazarov*, J.S. Jensen

Department of Mechanical Engineering, Solid Mechanics, Nils Koppels Alle, Technical University of Denmark, Building 404, 2800 Kgs. Lyngby, Denmark

Received 17 July 2007; received in revised form 31 August 2007; accepted 18 September 2007

Abstract

The aim of this article is to investigate the wave propagation in one-dimensional chains with attached non-linear local oscillators by using analytical and numerical models. The focus is on the influence of non-linearities on the filtering properties of the chain in the low frequency range. Periodic systems with alternating properties exhibit interesting dynamic characteristics that enable them to act as filters. Waves can propagate along them within specific bands of frequencies called pass bands, and attenuate within bands of frequencies called stop bands or band gaps. Stop bands in structures with periodic or random inclusions are located mainly in the high frequency range, as the wavelength has to be comparable with the distance between the alternating parts. Band gaps may also exist in structures with locally attached oscillators. In the linear case the gap is located around the resonant frequency of the oscillators, and thus a stop band can be created in the lower frequency range. In the case with non-linear oscillators the results show that the position of the band gap can be shifted, and the shift depends on the amplitude and the degree of non-linear behaviour.

Keywords: Non-linear wave propagation; Local resonators; Low-frequency band gaps

1. Introduction

The filtering properties of periodic structures with alternating characteristics have been investigated by many authors by using analytical, numerical and experimental methods. Such systems possess interesting filtering properties. Waves can propagate unattenuated along these structures within specific bands of frequencies called propagation or pass bands, and attenuate within bands of frequencies called stop bands, attenuation zones or band gaps. Band gaps in linear systems can also be created by introducing random inclusions or geometric disturbances. External excitation in such structures results in localised response surrounding the external input. The majority of the texts consider linear systems [1–3]. Localisation phenomena can also be observed in perfectly periodic non-linear structures [4–7], where spring–mass chains are studied and the non-linear behaviour is introduced either in the spring between the two neighbour masses, or by adding non-linear springs between the ground and the masses. The applications of these filtering phenomena are mainly in the high frequency range, as the distance between the inclusions has to be comparable with the wavelength.

In the beginning of the twentieth century Frahm discovered the vibration absorber as a very efficient way to reduce the vibration amplitude of machinery and structures by adding a spring with a small mass to the main oscillatory body [8]. The additional spring–mass system is tuned to be in resonance with the applied load. When the natural frequency of the attached absorber is equal to the excitation frequency, the main structure does not oscillate at all, as the attached absorber provides force equal and with opposite sign to the applied one. The idea can be exploited further by attaching multiple absorbers on a waveguide. Waves are attenuated in a frequency band located around the resonant frequency of the local oscillators, and thus stop bands can be created in the lower frequency range, which is often more important in mechanical applications. The effect has been studied experimentally and analytically in [9–11].

If the attached oscillators are non-linear, the response displays a dependency between the amplitude and the frequency. Very little is known about the filtering properties of the

* Corresponding author.
E-mail addresses: bsl@mek.dtu.dk (B.S. Lazarov), jsj@mek.dtu.dk (J.S. Jensen).

0020-7462/$ - see front matter © 2007 Elsevier Ltd. All rights reserved.
doi:10.1016/j.ijnonlinmec.2007.09.007

systems in this case. Periodic spring–mass system with attached non-linear pendulums are investigated in [12]. The attached pendulums are considered to be stiffer than the main chain, and they do not introduce band gaps in the lower frequency range. The aim of this paper is to investigate the behaviour of one-dimensional infinite spring–mass chain with locally attached oscillators with linear or non-linear behaviour. The oscillators are considered to be relatively soft compared to the main chain, and to create band gaps in the lower frequency range. The non-linearities in the attached oscillators are considered to be cubic. First the mechanical system together with the equations of motion is presented. The appearance of band gaps is shown in the linear case, and in the case with non-linear attached oscillators the method of harmonic balance is utilised to obtain a system of equations for the wave amplitude, as well as an approximate expression for the wave propagation properties of the chain. The analytical results are compared with the ones obtained by numerical simulations, some of which are presented in [13].

2. Mechanical system and equations of motion

The considered spring–mass system with attached local oscillators is shown in Fig. 1. Using the dynamic equilibrium condition for mass j, the equations describing its motion together with the equation of motion of the attached oscillator can be written as

$$(m+M)\frac{\mathrm{d}^2u_j}{\mathrm{d}\tau^2}+2ku_j-ku_{j-1}-ku_{j+1}+M\frac{\mathrm{d}^2q_j}{\mathrm{d}\tau^2}=0, \quad (1)$$

$$M\frac{\mathrm{d}^2q_j}{\mathrm{d}\tau^2}+c\dot{q}_j+k^l f(q_j)+M\frac{\mathrm{d}^2u_j}{\mathrm{d}\tau^2}=0, \quad (2)$$

where k is the spring stiffness between two masses, m is the mass at position $j=0,1,\ldots,\infty$, M is the mass of the attached local oscillator, $k^l f(q_j)$ is its restoring force and c is a viscous damping coefficient. u_j is the displacement of mass j, with positive direction shown in Fig. 1, and q_j is the relative displacement of the local oscillator. Both u_j and q_j are functions of the time and their positions j. The function $f(q_j)$ is assumed to be in the form

$$f(q_j)=q_j+\gamma_j q_j^3, \quad (3)$$

where γ_j is a parameter controlling the degree of non-linearity. By introducing normalised time $t=\omega_0\tau$, where $\omega_0=\sqrt{k/m}$, the coefficients $\beta=M/m$ and $\alpha=k^l/k$, Eqs. (1) and (2) can be written as

$$\ddot{u}_j+2u_j-u_{j-1}-u_{j+1}-\beta\kappa^2 f(q_j)-2\beta\zeta\kappa\dot{q}_j=0, \quad (4)$$

$$\ddot{q}_j+2\zeta\kappa\dot{q}_j+\kappa^2 f(q_j)+\ddot{u}_j=0, \quad (5)$$

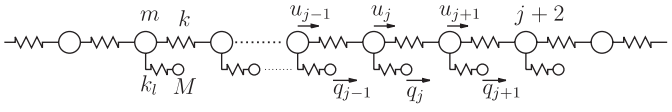

Fig. 1. Spring mass system with attached local oscillators.

where $\kappa=\sqrt{\alpha/\beta}$ and $\ddot{()}$ denotes the second derivative with respect to the normalised time t.

3. Band gaps in spring–mass chains with attached oscillators

3.1. Linear undamped oscillators

Using the idea for the vibration absorber, an efficient filter for waves propagating along a spring–mass chain can be created by attaching multiple absorbers to the chain as shown in Fig. 1. The equations of motion are given by (4) and (5), where the non-linear parameter γ and the damping parameter ζ are set to zero. In order to study the transmission properties of the chain, the solution is sought in the form [1]

$$u_j=B\mathrm{e}^{j\mu_u+\mathrm{i}\omega t}, \quad (6)$$

where μ_u is the so-called wave propagation constant of harmonic wave with frequency ω, which is equal to the wave number multiplied by the distance between the masses in the main chain, and j is the mass index. The displacements of the neighbour masses $j+1$ and $j-1$ become

$$u_{j+1}=\mathrm{e}^{\mu_u}u_j, \quad u_{j-1}=\mathrm{e}^{-\mu_u}u_j. \quad (7)$$

By inserting (6) and (7) into the equations of motion (4) and (5), and requiring the resulting equations to be valid at all time instances, the following relation between μ_u and ω is obtained:

$$\cosh(\mu_u)=1+\frac{1}{2}\frac{\omega^4-(1+\beta)\kappa^2\omega^2}{\kappa^2-\omega^2}. \quad (8)$$

Eq. (8) is also known as the dispersion relation. Plots of the real and the imaginary part of μ_u for different frequencies are shown in Fig. 2. Around the natural frequency of the attached oscillators there exists a frequency band where waves are attenuated. Outside the band gap, two neighbour masses j and $j+1$ oscillate with phase difference $\mathrm{Im}(\mu_u)$. Inside the band gap, below the natural frequency κ of the attached oscillators, two neighbour masses oscillate with an opposite phase $\mathrm{Im}(\mu_u)=\pi$ and above κ they oscillate with phase difference $\mathrm{Im}(\mu_u)=0$. The real part $\mathrm{Re}(\mu_u)$ gives the attenuation rate of the wave amplitude. At $\omega=\kappa$ the real part of μ_u is infinity and decreases to zero outside the band gap. It should be pointed out that the system studied in this section has no energy dissipation mechanism.

3.2. Non-linear local oscillators

A solution of the non-linear system of equations (4) and (5) is not known in a closed form. An approximate solution can be obtained by using the method of harmonic balance, the method of multiple scales or the method of averaging, e.g. [14,15]. Non-linear oscillators with third order non-linearities, as the one described by (5), are well studied in the literature. Based on these solutions the method of harmonic balance is applied here, in order to study the wave propagation along the chain with attached damped non-linear oscillators.

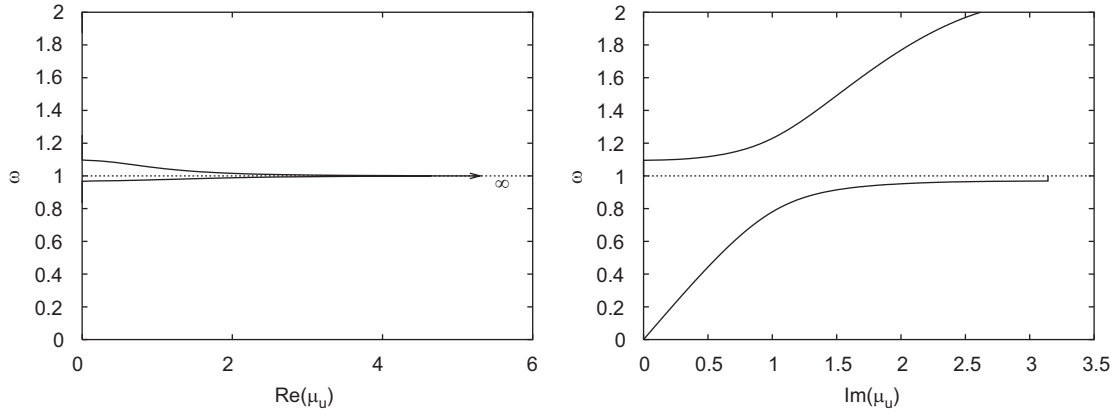

Fig. 2. Dispersion relation for $\kappa = 1.0$ and $\beta = 0.1$.

The time response of $q_j(t)$ is assumed to be periodic in the form of complex Fourier series

$$q_j(t) = \sum_k \varepsilon^{(k-1)/2} A_{k,j} e^{ik\omega t} + \varepsilon^{(k-1)/2} \bar{A}_{k,j} e^{-ik\omega t}, \quad k = 1, 3, \ldots, \tag{9}$$

where ε is a dimensionless bookkeeping parameter showing the order of the amplitude of the motion. By substituting (9) into (5) and integrating twice with respect to time, the following expression for the time response of mass j can be obtained:

$$u_j(t) = A_{1,j}\left(-1 + \frac{\kappa^2}{\omega^2} + 3\varepsilon\frac{\gamma_j\kappa^2}{\omega^2}A_{1,j}\bar{A}_{1,j} + \frac{2i\zeta\kappa}{\omega}\right)e^{i\omega t} + \varepsilon\left(-A_{3,j} + \frac{2}{3}\frac{i\zeta\kappa}{\omega}A_{3,j} + \frac{1}{9}\frac{\kappa^2}{\omega^2}A_{3,j} + \frac{1}{9}\frac{\gamma_j\kappa^2}{\omega^2}A_{1,j}^3\right) \times e^{i3\omega t} + \text{c.c.} + O(\varepsilon^2). \tag{10}$$

The expression in the above equation is obtained by truncating the time series and preserving only the first two terms. By substituting (10) and (9) into (4) and equating to zero the coefficients in front of $e^{ik\omega t}$, a system of algebraic equations for the amplitudes $A_{k,j}$ can be obtained

$$\left(2\left(\frac{\kappa^2}{\omega^2} - 1\right) + \omega^2 - \beta_1\kappa^2 + 2i\zeta\frac{\kappa}{\omega}(2 - \beta_1\omega^2)\right)A_{1,j} + 3\gamma_j\frac{\kappa^2}{\omega^2}(2 - \beta_1\omega^2)A_{1,j}^2\bar{A}_{1,j} + \left(1 - \frac{\kappa^2}{\omega^2} - 2i\zeta\frac{\kappa}{\omega}\right)(A_{1,j+1} + A_{1,j-1}) - 3\gamma_{j+1}\frac{\kappa^2}{\omega^2}A_{1,j+1}^2\bar{A}_{1,j+1} - 3\gamma_{j-1}\frac{\kappa^2}{\omega^2}A_{1,j-1}^2\bar{A}_{1,j-1} = 0, \tag{11}$$

$$\left(2\left(\frac{\kappa^2}{\omega_3^2} - 1\right) + \omega_3^2 - \beta_1\kappa^2 + 2i\zeta\frac{\kappa}{\omega_3}(2 - \beta_1\omega_3^2)\right)A_{3,j} + \left(2\frac{\kappa^2}{\omega_3^2} - \beta_1\kappa^2\right)\gamma_j A_{1,j}^3 + \left(1 - \frac{\kappa^2}{\omega_3^2} - 2i\zeta\frac{\kappa}{\omega_3}\right) \times (A_{3,j+1} + A_{3,j-1}) - \gamma_{j+1}\frac{\kappa^2}{\omega_3^2}A_{1,j+1}^3 - \gamma_{j-1}\frac{\kappa^2}{\omega_3^2}A_{1,j-1}^3 = 0, \tag{12}$$

where $\beta_1 = \beta + 1$ and $\omega_3 = 3\omega$. By specifying the amplitudes for two neighbour masses and, respectively, for the attached oscillators, a solvable system of equations for the response amplitudes of the attached oscillators can be obtained. The system is non-linear and there can be multiple solutions satisfying it in certain cases. The amplitude of the wave travelling along the main chain can be obtained by inserting the amplitude of the attached oscillators into (10).

The wave travelling along the spring–mass chain can also be investigated by using the wave number multiplied by the distance between the masses in the main chain μ_u. The displacements of the masses neighbour to mass j can be expressed as

$$u_{j\pm1} = \sum_k B_{k,j} e^{\pm\mu_{u_k}} e^{ik\omega t} + \text{c.c.}, \tag{13}$$

where $B_{k,j}$ are the coefficients in front of $e^{ik\omega t}$ from Eq. (10). It can be clearly seen that the solution in the non-linear case consists of a zero order wave with frequency ω and additional high order waves. As the non-linearities are assumed to be small and the focus is on the filtering properties of the chain around the linear natural frequency of the attached oscillators, the contributions to the solution of the harmonics of order equal to and higher than $k = 3$ are neglected. Substituting (13) and (9) into (4), equating the coefficients in front of $e^{i\omega t}$ to zero and solving the resulting equation with respect to μ_u, the dispersion relation for the non-linear case is obtained in

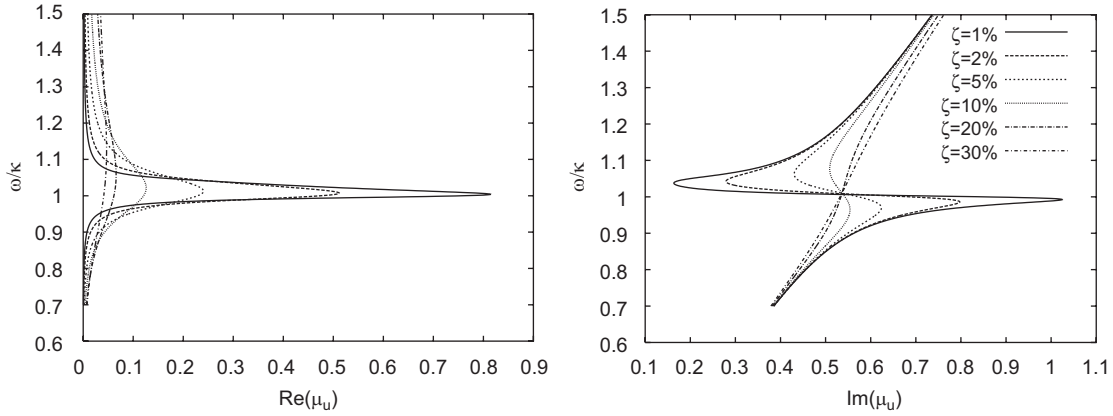

Fig. 3. Dispersion relation for $\beta = 0.1$, $\gamma = 0$ and different damping ratios.

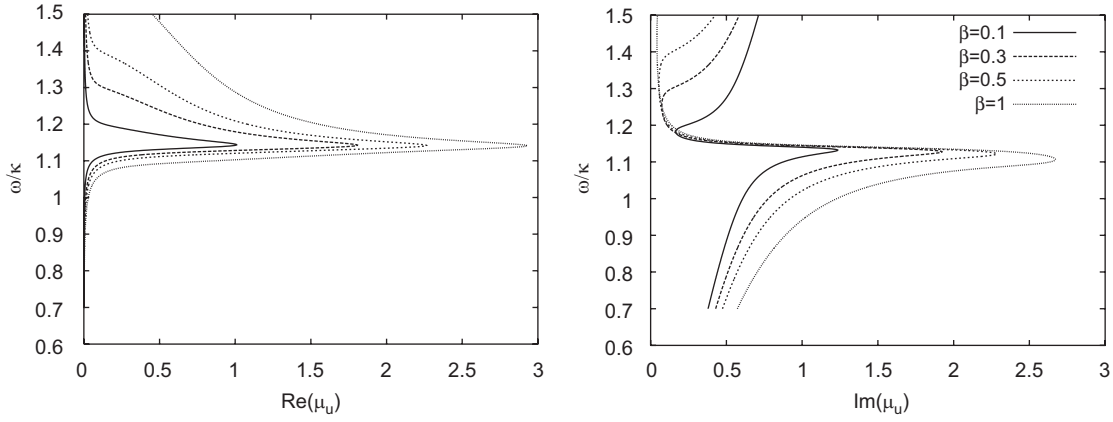

Fig. 4. Dispersion relation for $\zeta = 0.01$, $\gamma A_{1,j}\bar{A}_{1,j} = 0.1$ and different mass ratios.

the form

$$\cosh(\mu_u) = 1 - \frac{1}{2}\omega^2 - \frac{1}{2}\frac{\omega^2\beta(\kappa^2 + 2i\zeta\kappa\omega + 3\kappa^2\gamma_j A_{1,j}\bar{A}_{1,j})}{(\kappa^2 + 2i\zeta\kappa\omega + 3\kappa^2\gamma_j A_{1,j}\bar{A}_{1,j} - \omega^2)}. \quad (14)$$

The dispersion relation for the linear case can be obtained from (14) by setting the non-linear parameter γ_j equal to zero and removing the damping in the attached oscillators. The influence of the damping parameter ζ on the dispersion relation in the linear case can be seen in Fig. 3. Den Hartog has shown in [8] that the introduction of viscous damping in the vibration absorber increases the frequency interval in which the device is effective. Similar behaviour can be observed for wave propagation problems. The maximal value of the attenuation rate decreases with increasing the damping in the attached oscillators, and for high values of ζ the band gap practically disappears. Similar behaviour is observed for two-dimensional wave propagation problems in [16]. The value of $\mathrm{Im}(\mu_u)$ is always different from 0 or $\pm\pi$ in the damped case, and thus oscillatory behaviour in the spatial domain can always be observed. The influence of the mass ratio β on the band gap is shown in Fig. 4. The width of the stop band can be increased by increasing the attached mass.

For the non-linear spring–mass chain, μ_u depends on the amplitude of the attached oscillator at position j. Plots of the dispersion relation for different values of the non-linear parameter $\gamma A_{1,j}\bar{A}_{1,j}$ are shown in Fig. 5. As can be seen, the position of the maximal value of the attenuation rate varies with the value of the non-linear parameter. The maximum is shifted above the linear natural frequency of the attached oscillators, and the shift increases for larger values of the amplitude $A_{1,j}$. For a negative value of the non-linear parameter γ, the shift will occur in the opposite direction, below the linear natural frequency. As the wave propagates, the amplitude $A_{1,j}$ decreases, due to the reflections from the attached oscillators, as well as due to the damping in the system, and the position of the maximal value of $\mathrm{Re}(\mu_u)$ moves toward $\omega/\kappa = 1$. The amplitudes vary along the chain, and μ_u becomes a function of the spatial coordinate j. A fixed wave propagation constant cannot be defined in the non-linear case.

3.3. Transmission properties based on analytical calculations

For given values of the amplitudes $B_{1,j}$ and $A_{1,j}$ of mass j and the corresponding attached oscillator, the value of μ_u can be calculated using (14). The amplitude of the mass at position $j+1$ is calculated as $B_{1,j+1} = e^{\mu_u} B_{1,j}$. The amplitude

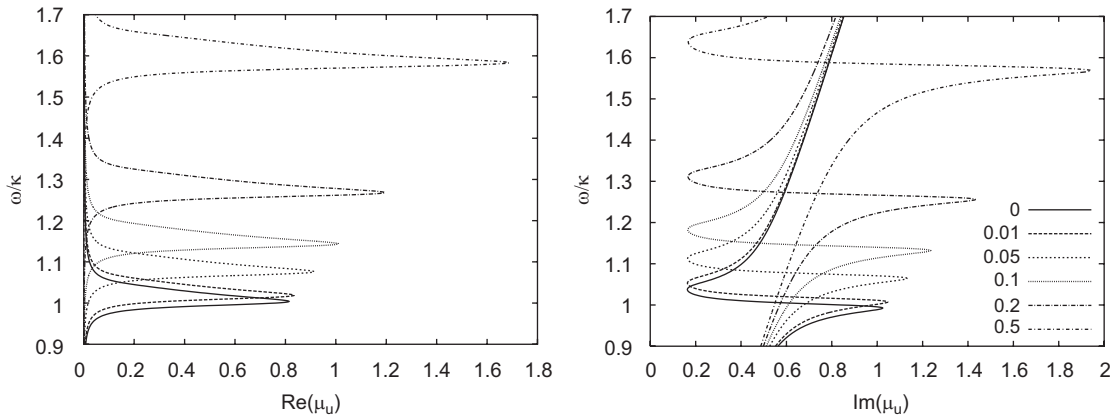

Fig. 5. Dispersion relation for $\beta = 0.1$, $\zeta = 0.01$ and different values of the non-linear parameter $\gamma A_{1,j}\bar{A}_{1,j}$.

$A_{1,j+1}$ of the attached oscillator can be calculated by solving the following equation:

$$B_{1,j+1}=A_{1,j+1}\left(-1+\frac{\kappa^2}{\omega^2}+3\frac{\gamma_{j+1}\kappa^2}{\omega^2}A_{1,j+1}\bar{A}_{1,j+1}+\frac{2\mathrm{i}\zeta\kappa}{\omega}\right) \tag{15}$$

which is obtained from (10) and (13) by equating the coefficients of $e^{i\omega t}$. Eq. (15) resembles the equation for the amplitude of the stationary response of externally excited Duffing oscillator. By using polar representation for the amplitudes $A_{1,j+1} = R_A(\cos(\psi) + \mathrm{i}\,\sin(\psi))$ and $R_B = |B_{1,j+1}|$, (15) can be written as

$$9\gamma^2 r^4 R_A^6 + 6\gamma_{j+1} r^2 (r^2-1) R_A^4 + ((r^2-1)^2 + 4\zeta^2 r^2) R_A^2 - R_B^2 = 0, \tag{16}$$

where $r = \kappa/\omega$. Eq. (16) can be represented as a cubic equation with respect to R_A^2. It has either one, or three real roots for R_A^2. In the second case, two of the solutions are stable and one of them is unstable, which is well known property of the Duffing oscillator [14]. There are two values of μ_u corresponding to the two stable solutions of (16), and a unique value for $B_{1,j+2}$ cannot be obtained. The two solutions for $\mu_{u,j+1}$ can be ordered by the magnitude of their real part. The one with larger absolute real value, $\mu^l_{u,j+1}$, produces an amplitude with a smaller absolute value, and the other one, $\mu^u_{u,j+1}$, produces an amplitude with a larger absolute value. Continuing in this way, an estimate for the upper and the lower bounds of the absolute value of the wave amplitude can be obtained:

$$|B^u_{1,j+k}| = \left(\prod_{n=1\ldots k} e^{\mathrm{Re}(\mu^u_{u,j+n})}\right)|B^u_{1,j}|,$$

$$|B^l_{1,j+k}| = \left(\prod_{n=1\ldots k} e^{\mathrm{Re}(\mu^l_{u,j+n})}\right)|B^l_{1,j}|. \tag{17}$$

In the case where only a single real solution for R_A^2 exists, $\mu^l_{u,j+k}$ is equal to $\mu^u_{u,j+k}$ and $|B^u_{1,j+k}| = |B^l_{1,j+k}|$.

4. Numerical simulations

The theoretical analysis derived in the previous section is validated by using numerical simulations for finite spring–mass chain, as shown in Fig. 1. Absorbing boundary conditions are applied at each end of the chain by adding dash-pot with a damping constant $c = 1$. The damping constant corresponds to the exact absorbing boundary condition for a continuous rod with distributed mass $\rho A = 1$ and stiffness $EA = 1$, where ρ is the mass density, A is the section area and E is the elastic modulus. A wave travelling in the right direction is generated by applying a harmonic force with frequency ω and unit amplitude at the left end of the chain. The first and the last 10 masses in the chain are without attached oscillators. The wave travels undisturbed, until it reaches the part with the attached oscillators, where a part of it is reflected back, and a part of it propagates until it reaches the right end of the chain. The system is integrated numerically, until steady state is reached. The root-mean-squared (RMS) value of the response amplitude

$$[B_j] = \frac{1}{\sqrt{2}}\sqrt{\frac{1}{T}\int_t^{t+T} u_j^2(t)\,\mathrm{d}t} \tag{18}$$

is calculated at the right end of the chain and is compared with the results obtained by using the analytical prediction derived in the previous section. The RMS value is calculated for a finite time interval $T = 20\lambda$, where $\lambda = 2\pi/\omega$ and ω is the frequency of the generated wave. The contribution of the higher order harmonics to the RMS value of the response amplitude is assumed to be small.

4.1. Influence of the non-linearities

The transmission properties of a chain with 2000 attached oscillators calculated by using numerical simulations, and the procedure in Section 3.3, are shown in Fig. 6. The non-linear coefficients $\gamma_j = \gamma$ are taken to be the same for all attached oscillators. The results are obtained for several values of γ. The linear normalised frequency κ of the attached oscillators is 0.05. For small values of the non-linear coefficient the estimated

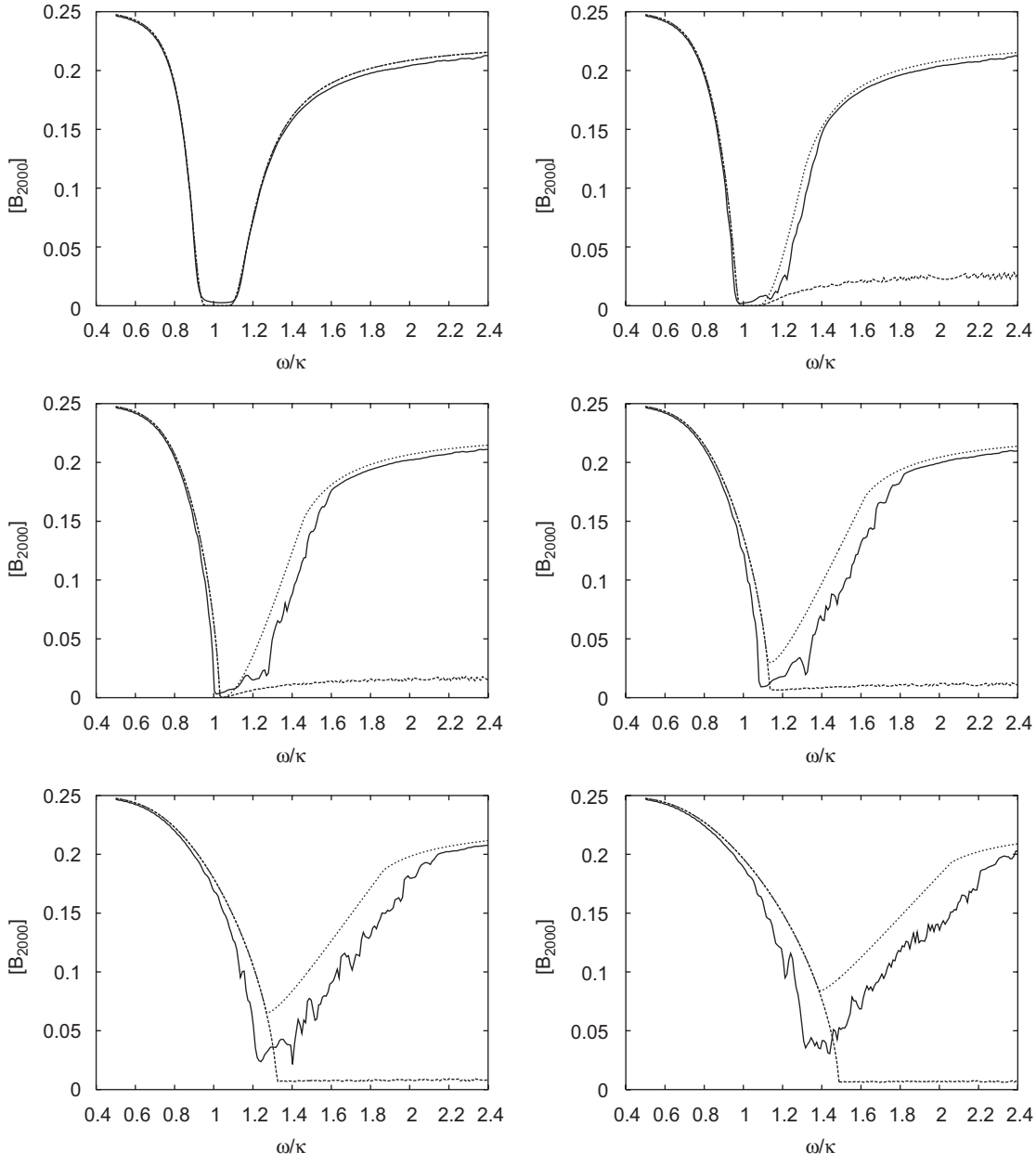

Fig. 6. Comparison of the theoretical prediction (dotted curves) of the transmitted amplitude with the one obtained by numerical integration for different values of $\gamma = 0.0, 0.1, 0.25, 0.5, 1.0, 1.5$, $\beta = 0.1$, $\zeta = 0.01$. The RMS value of the amplitude of the first mass is 0.25.

upper and lower values of the absolute value of the amplitude bound well the estimated RMS value of the amplitude from the numerical simulations. For large values of the non-linearity the results start to deviate. The frequency shift in the band gap can be clearly observed in all plots for $\gamma \neq 0$. In addition, the shape of the band gap changes, and the decaying rate decreases with increasing the non-linear coefficient.

4.2. Influence of the chain length

The results obtained by both numerical simulations and analytical calculations for chains with different number of the attached oscillators are shown in Fig. 7. The non-linear parameter $\gamma = 0.3$ is kept at a fixed value for all different spring–mass chains, and is taken to be the same for all attached oscillators. As can be seen, for small number of the attached oscillators the frequency shift of the band gap is significant. The reduction of the transmitted amplitude is relatively small compared with the one obtained for larger number of the attached oscillators. As the wave propagates along the chain, the amplitude is decreasing leading to frequency shift of the band gap back towards the linear natural frequency. The effect can be clearly observed by studying the plots.

4.3. Chains with variable non-linear coefficients

If the wave frequency is located in the band gap, the amplitude is decaying fast, and the band gap is shifted back to

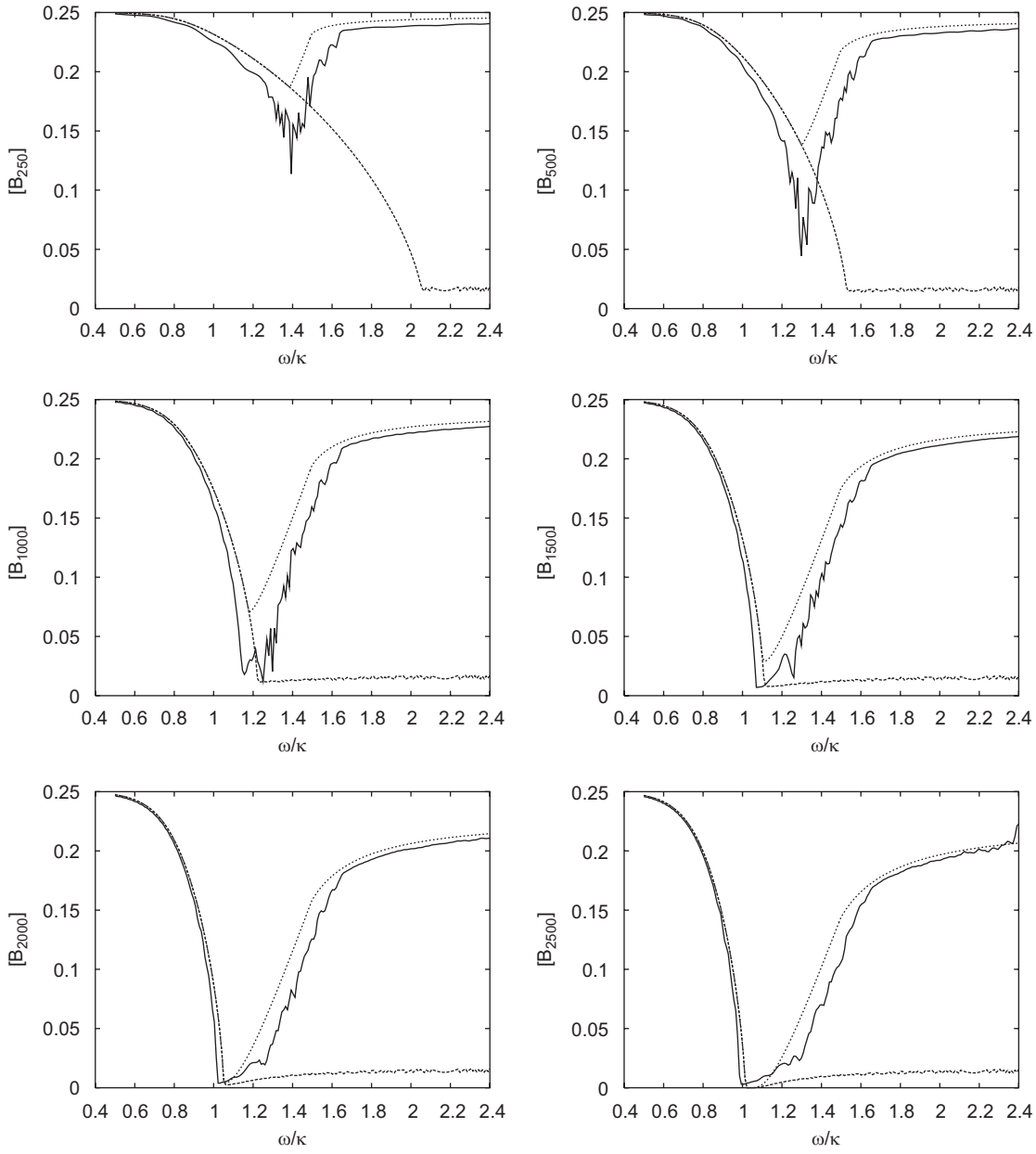

Fig. 7. Comparison of the theoretical prediction (dotted curve) of the transmitted amplitude with the one obtained by numerical integration for different numbers of the attached oscillators $n_l = 250, 500, 1000, 1500, 2000, 2500$ and $\gamma = 0.3$.

the one obtained for linear attached oscillators. The shift depends on the value of $\gamma_j A_{1,j} \bar{A}_{1,j}$. As the amplitude decreases along the chain, γ_j can be changed, in order to keep the shift of the band gap at a desirable frequency. For very small amplitudes the value of γ needs to be very large and thus, there will always be a wave with finite amplitude propagating after the part of the chain with attached oscillators. Plots of the transmitted amplitude for chains with 400 attached oscillators are shown in Fig. 8. A chain with variable non-linearities is chosen with γ equal to $0.12\sqrt{\exp((i-1)/100)}$, and for comparison the results for chains with constant $\gamma = 0.12$ corresponding to the minimal value of γ in the chain with variable non-linearities, $\gamma = 0.88$ (maximal value) and $\gamma = 0.3$ (intermediate value), are shown in the figure. The input RMS value of the amplitude is equal to 0.25, the damping coefficient is $\zeta = 0.02$ and i is the number of the attached oscillators. The theoretical prediction is calculated by using the procedure in Section 3.3. In all cases with $\gamma \neq 0$, a shift in the stop band frequency can be clearly observed. The shift of the chain with variable γ is between the shift for the cases with $\gamma = 0.12$ and 0.88, and close to the case with the intermediate value $\gamma = 0.3$. The theoretical prediction indicates better filtering properties in the case with variable γ and this result is also supported by the numerical simulations.

The expression for γ in the chain with variable non-linearities is obtained by trial and error. A systematic optimisation procedure can produce better results. More improvements are

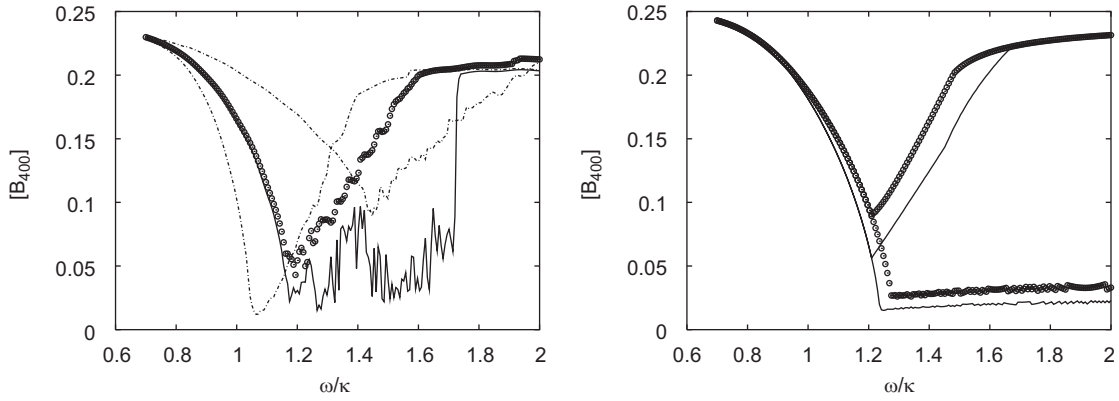

Fig. 8. Comparison of the transmitted amplitude for variable (solid line) and fixed (circular dots $\gamma = 0.3$) γ for chain with 400 attached oscillators. The two dashed lines show the transmitted amplitude for fixed γ (0.12, 0.88) equal to the lowest and the highest value used for the chain with varying non-linearities. The second plot is obtained by using the analytical calculations with variable γ and $\gamma = 0.3$.

possible if variation is allowed not only in the non-linearities but also in the linear stiffness coefficients, mass ratio and the damping. A study based on a topology optimisation approach for a similar linear continuous system is presented by the authors in [17]. An extension to the non-linear case is a subject for future work.

5. Conclusions

The focus in this article is on the influence of the non-linearities on the filtering properties of the chain around the linear natural frequency of the attached oscillators. The position of the band gap can be shifted by changing the degree of non-linearity of the oscillators, or by changes of the wave amplitude. A comparison with numerical simulations for a finite chain with attached oscillators shows that the analytical predictions match simulations well for small non-linearities, and start to deviate for large ones. Both estimations clearly show a shift in the band gap. The transmitted amplitude will always be different than zero for wave frequencies different than the linear natural frequency of the attached oscillators and for finite values of the non-linear parameter γ. The change in the position of the stop band can be utilised in the design of adjustable filters in the lower frequency range. The optimal distribution of the non-linearities, as well as the natural frequencies and the damping of the attached oscillators, is subject to further investigations.

Acknowledgements

This work was supported by Grant 274-05-0498 from the Danish Research Council for Technology and Production Sciences. The authors wish to thank Professor Jon Juel Thomsen for his suggestions and valuable discussions.

References

[1] L. Brillouin, Wave Propagation in Periodic Structures, Dover Publications Inc., New York, 1953.
[2] D.J. Mead, Wave-propagation and natural modes in periodic systems. 1. Mono-coupled systems, J. Sound Vib. 40 (1975) 1–18.
[3] D.J. Mead, Wave-propagation and natural modes in periodic systems. 2. Multi-coupled systems, with and without damping, J. Sound Vib. 40 (1975) 19–39.
[4] A.F. Vakakis, M.E. King, A.J. Pearlstein, Forced localization in a periodic chain of nonlinear oscillators, Int. J. Non-linear Mech. 29 (1994) 429–447.
[5] G. Chakraborty, A.K. Mallik, Dynamics of a weakly non-linear periodic chain, Int. J. Non-linear Mech. 36 (2001) 375–389.
[6] A. Marathe, A. Chatterjee, Wave attenuation in nonlinear periodic structures using harmonic balance and multiple scales, J. Sound Vib. 289 (2006) 871–888.
[7] O. Richoux, C. Depollier, J. Hardy, Propagation of mechanical waves in a one-dimensional nonlinear disordered lattice, Phys. Lett. E 73 (2006) 026611.
[8] J.P. Den Hartog, Mechanical Vibrations, 4th ed., McGraw-Hill, New York, 1956 (Reprinted by Dover Publications Inc., New York, 1985).
[9] D.L. Yu, Y.Z. Liu, G. Wang, L. Cai, J. Qiu, Low frequency torsional vibration gaps in the shaft with locally resonant structures, Phys. Lett. A 348 (2006) 410–415.
[10] Z. Liu, X. Zhang, Y. Mao, Y.Y. Zhu, Z. Yang, C.T. Chan, P. Sheng, Locally resonant sonic materials, Science 289 (2000) 1734–1736.
[11] G. Wang, J. Wen, X. Wen, Quasi-one-dimensional phononic crystals studied using the improved lumped-mass method: application to locally resonant beams with flexural wave band gap, Phys. Lett. B 71 (2005) 104302.
[12] I.T. Georgiou, A.F. Vakakis, An invariant manifold approach for studying waves in a one-dimensional array of non-linear oscillators, Int. J. Non-Linear Mech. 31 (1996) 871–886.
[13] B.S. Lazarov, J.S. Jensen, Band gap effects in spring–mass chains with attached local oscillators, in: Proceedings of the ECCOMAS Thematic Conference of Computational Methods in Structural Dynamics and Earthquake Engineering, Rethymno, Crete, Greece, 2007.
[14] J.J. Thomsen, Vibrations and Stability, Springer, Berlin, Heidelberg, 2003.
[15] A.H. Nayfeh, D.T. Mook, Nonlinear Oscillations, Wiley, New York, 1979.
[16] J.S. Jensen, Phononic band gaps and vibrations in one- and two-dimensional mass–spring structures, J. Sound Vib. 266 (2003) 1053–1078.
[17] J.S. Jensen, B.S. Lazarov, Topology optimization of distributed mass dampers for low-frequency vibration suppression, in: Proceedings of the ECCOMAS Thematic Conference of Computational Methods in Structural Dynamics and Earthquake Engineering, Rethymno, Crete, Greece, 2007.